Gravitational and collective effects in an output coupler for a Bose-Einstein condensate in an atomic trap

Weiping Zhang[1] and D. F. Walls[2]
[1]*School of Mathematics, Physics, Computing, and Electronics, Macquarie University, Sydney, New South Wales 2109, Australia*
[2]*Physics Department, University of Auckland, Private Bag 92019, Auckland, New Zealand*
(Received 15 September 1997)

A three-component vector quantum field theory is developed to describe the electronic-spin-resonance interaction of a magnetically trapped Bose-Einstein condensate with a radio frequency field. The theory is directly applied to simulate the recent experiment of Mewes *et al.* for an output coupler for a Bose-Einstein condensate in a magnetic trap [Phys. Rev. Lett. **78**, 582 (1997)]. By employing the mean-field approach, we study the collective dynamics of the multicomponent matter field via the nonlinear Schrödinger equation. Including the effect of gravity, we study the spin-resonance Rabi oscillations for the three-component Bose-Einstein condensate in three ground-state hyperfine levels and simulate the dynamic expansion of the condensate components coupled out of the magnetic trap. [S1050-2947(98)00602-7]

PACS number(s): 03.75.Fi, 05.30.Jp, 32.80.Pj, 67.90.+z

The recent realizations of Bose-Einstein condensation in a magnetically trapped gas of ultracold alkali-metal atoms [1–3] have generated both experimental and theoretical interest in studying the properties of Bose-Einstein condensates (BEC) and manipulating such coherent matter by electromagnetic fields. For example, the research on the collective excitation of BEC [4–6], the weak light scattering of BEC [7–13], quantum dynamics of BEC [14], and laser manipulation of BEC [15,16], etc., has explored different aspects of such coherent atomic samples. Recently, manipulation of BEC by radio frequency (rf) fields has been demonstrated experimentally by Mewes *et al.* [17]. In this experiment, the trapped condensate is coupled to a rf pulse field. The spin-flip transition results in the partial leakage of the condensate from the trap. As a result, the rf pulse field can coherently ''split'' the condensate into three different pieces: one still stays in the trap and the others may escape from the trap and propagate along the direction of gravity in free space. The operation is similar to an optical beam splitter or coupler for photons. The pulsed radio frequency field acts as a beam splitter or coupler for the atoms in the trap. Therefore Mewes *et al.* have achieved an output coupler for Bose-condensed atoms and regard it as a rudimentary version of a pulsed atom laser since the output atomic wave packets are from a coherent matter source.

The coherent transfer or coupling of BEC has been studied theoretically for a coherent atomic beam splitter [18] and also for trapped ground-state alkali-metal atoms with two different hyperfine sublevels [19,20]. However, a quantitative description including gravity and collective dynamics in three-dimensional (3D) space for the coherent coupling of BEC with multihyperfine sublevels has not yet been done. In this paper, our purpose is to develop such a quantitative theory for the multicomponent coherent matter field interacting with a rf field. We then employ the theory to give a realistic simulation of processes in the output coupler experiment done by Mewes *et al.* A schematic diagram in Fig. 1 displays the system considered in this paper. Figure 1(a) shows the hyperfine manifold for $F=1$ ground-state alkali atoms in a static magnetic field. We assume that initially BEC is prepared in the trapped Zeeman level $m_F=-1$. When a rf field is applied to the system, by spin-flip transitions, the condensate will be coupled to the Zeeman levels $m_F=0$ and $m_F=1$, which are untrapped. The untrapped condensate components will leave from the trapping regime under gravity. To quantitatively describe the coupling process, we begin by treating the Bose-condensed atoms in the alkali ground state $F=1$ as a three-component vector atomic field,

$$\psi(\vec{r},t)=\sum_{m_F=-1}^{m_F=1}\psi_{m_F}(\vec{r},t)|F=1,m_F\rangle, \tag{1}$$

where the operator $\psi_{m_F}(\vec{r},t)$ corresponds to the atomic field component in the magnetic Zeeman level m_F. The Hamiltonian for the coupling of the atomic field to the rf field can be expressed as

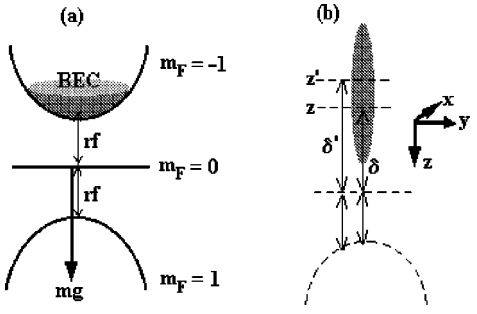

FIG. 1. (a) Schematic diagram for coherent coupling of the trapped condensate component to the untrapped condensate components by a rf field. (b) The pencil-shaped condensate where different spatial positions in the axial direction correspond to different detuning due to gravitational inhomogeneities.

$$H=\int d^3r\ \psi^{\dagger}(\vec{r})\left(-\frac{\hbar^2\nabla^2}{2m}-\mu+H_0-\vec{\mu}_M\cdot\vec{B}_R\right)\psi(\vec{r})+\frac{1}{2}\int d^3r_a\int d^3r_b\psi^{\dagger}(\vec{r}_a)\psi^{\dagger}(\vec{r}_b)\hat{V}(\vec{r}_a-\vec{r}_b)\psi(\vec{r}_b)\psi(\vec{r}_a), \tag{2}$$

where μ is the chemical potential of the gas, H_0 is the internal free Hamiltonian for the atoms in the trapping magnetic fields and gravitational field, $\vec{\mu}_M$ is the magnetic dipole moment of the atoms, and $\vec{B}_R$ the rf magnetic field. The second term in Eq. (2) describes the collective excitations of atoms due to the interatomic interaction, which has the simple form in the pseudopotential approximation [21,22]

$$\hat{V}(\vec{r}_a-\vec{r}_b)=\frac{4\pi\hbar^2a_s}{m}\ \delta(\vec{r}_a-\vec{r}_b)P_s+\frac{4\pi\hbar^2a_T}{m}\ \delta(\vec{r}_a-\vec{r}_b)P_T, \tag{3}$$

where a_s and a_T are the s-wave scattering lengths for the singlet- and triplet-state atomic collisions, respectively. P_s and P_T are the corresponding projection operators on the singlet and triplet subspaces. In terms of Eq. (2), we have the following nonlinear Schrödinger equations for the coherent coupling of the vector atomic field to the rf magnetic field in the interaction picture

$$\begin{aligned}
i\hbar\frac{\partial\psi_1}{\partial t}&=\left(-\frac{\hbar^2\nabla^2}{2m}-\mu+\hbar\Delta\omega+V_1(\vec{r})\right)\psi_1-\frac{\hbar\omega_R}{\sqrt{2}}\ \psi_0+\hbar\kappa[\rho(\vec{r})+\psi_1^{\dagger}\psi_1]\psi_1-2\hbar\chi\psi_{-1}^{\dagger}\psi_{-1}\psi_1+\hbar\chi\psi_{-1}^{\dagger}\psi_0^2,\\
i\hbar\frac{\partial\psi_0}{\partial t}&=\left(-\frac{\hbar^2\nabla^2}{2m}-\mu+V_0(\vec{r})\right)\psi_0-\frac{\hbar\omega_R}{\sqrt{2}}\ (\psi_1+\psi_{-1})+\hbar\kappa[\rho(\vec{r})+\psi_0^{\dagger}\psi_0]\psi_0-2\hbar\chi\psi_0^{\dagger}\psi_0\psi_0+2\hbar\chi\psi_0^{\dagger}\psi_1\psi_{-1},\\
i\hbar\frac{\partial\psi_{-1}}{\partial t}&=\left(-\frac{\hbar^2\nabla^2}{2m}-\mu-\hbar\Delta\omega+V_{-1}(\vec{r})\right)\psi_{-1}-\frac{\hbar\omega_R}{\sqrt{2}}\ \psi_0+\hbar\kappa[\rho(\vec{r})+\psi_{-1}^{\dagger}\psi_{-1}]\psi_{-1}-2\hbar\chi\psi_1^{\dagger}\psi_1\psi_{-1}+2\hbar\chi\psi_1^{\dagger}\psi_0\psi_0,
\end{aligned} \tag{4}$$

where $\Delta\omega$ is the detuning of the radio frequency field from the atomic resonance at the center of the trap, $\omega_R=\mu_B g_F B_R/2\hbar$ is the rf Rabi frequency, which describes the spin-flip transitions between Zeeman levels. The nonlinear terms in Eqs. (4) describe the collective effects due to interatomic interactions with the nonlinear coefficients defined as $\kappa=\hbar\pi(3a_s+13a_T)/(4m)$ and $\chi=\hbar\pi(a_T-a_s)/(4m)$. The total density operator of the gas is denoted as $\rho(\vec{r})=\Sigma_{j=-1}^{1}\psi_j^{\dagger}(\vec{r})\psi_j(\vec{r})$. The external potentials in Eqs. (4) due to the trapping magnetic field, the gravitational field, and the compensation magnetic field for gravity have the expressions

$$\begin{aligned}
V_{-1}&=m\omega^2(x^2+y^2)/2+m\omega_z^2z^2/2,\\
V_0&=-mgz,\\
V_1&=-m\omega^2(x^2+y^2)/2-m\omega_z^2z^2/2-2mgz.
\end{aligned} \tag{5}$$

Equations (4) and (5) determine the coherent coupling dynamics of the Bose-condensed gas in the rf field. In general, it is difficult to solve these nonlinear coupled quantum field equations even by numerical methods. Here we employ the mean-field approach to these quantum field operators in Eqs. (4) so that they can be treated as macroscopic wave functions for the condensate components. In this case, Eqs. (4) are simplified to the nonlinear coupled wave equations for the condensate wave functions. We employ these nonlinear coupled wave equations to simulate the output coupler for the BEC demonstrated by Mewes *et al.* [17]. The numerical simulation is divided into two steps. The first step is to study the Rabi oscillation in the coherent coupling of the condensate to the rf pulse field. The second is to simulate the free expansion and propagation of the output condensate components including the collective interatomic interactions and the external potentials given in Eqs. (5). The initial condensate chosen for our simulation is the pencil-shaped condensate used in the Mewes *et al.* experiment [see Fig. 1(b)]. The condensate is prepared in the trapped state $m_F=-1$ by a trapping potential, which is cylindrically symmetrical with an axial trapping frequency 18 times less than the radical trapping frequency [4]. The condensate has a length in the axial direction (gravity direction) that is about 20 times larger than its width in the radical direction [4]. In the output coupler experiment, Mewes *et al.* studied two different cases. In one they realized the coherent transfer of the initially trapped condensate to the untrapped components by sweeping the rf field through resonance. In the other they used monochromatic rf pulses to achieve the coherent transfer. We limit our discussions to the latter case with a single rf pulse. The rf pulse used in the experiment [17] has a duration about 6.6 μs, which is short enough to ignore the quantum dispersion due to the kinetic energy term during the interaction of the condensate with the rf pulse field. This enables us to adopt the standard Runge-Kutta method to numerically solve the nonlinear coupled wave equations (4) for different spatial-temporal points $(\vec{r}_i,t_i)$. In Fig. 2 we present the numerical result for the Rabi oscillation of the trapped fraction of the condensate for the same conditions as given in Ref. [17] for different amplitudes of the rf pulse. The frequency of the rf pulse is chosen to be resonant with the center of the trap $(\Delta\omega=0)$. The precision of the experimental data is insufficient to allow us to distinguish between the numerical

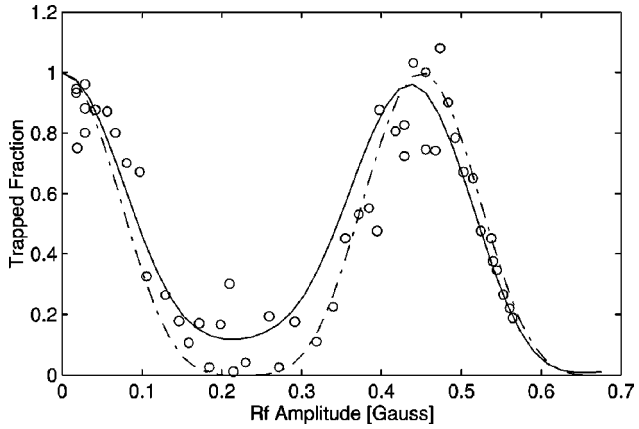

FIG. 2. Comparison of the numerical simulation for the Rabi oscillations of the trapped fraction in state $m_F=-1$ with the experimental data of Mewes *et al.*: the solid curve corresponds to the numerical result, the circle to the experimental data, and the dashed-dotted curve to the single-atom resonant Rabi solution.

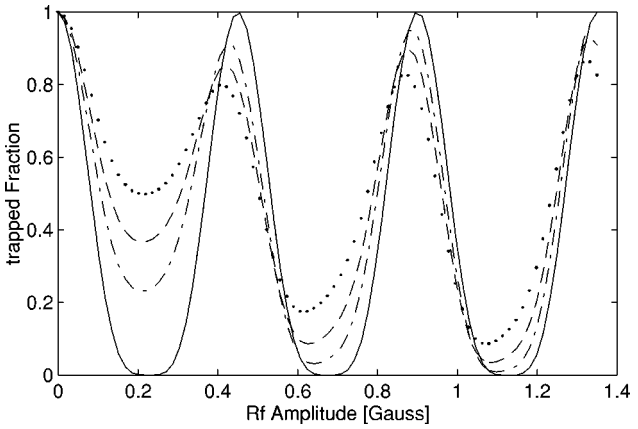

FIG. 3. Dependence of the Rabi oscillations of the trapped fraction in state $m_F=-1$ on the gravitational inhomogeneity: the solid curve is the single-atom resonant Rabi solution, the dashed-dotted curve corresponds to an initial condensate with an axial length 10 μm, the dashed curve to 20 μm, and the dotted curve to 30 μm.

curve (solid line) and the resonant single-atom Rabi solution $\cos^4(\omega_R t/2)$ (dashed-dotted line). To understand the deviation of both the experimental data and the numerical result from the resonant single-atom Rabi solution, we seek approximately analytic solutions for Eqs. (4) by assuming that the nonlinear terms slowly vary with time. This yields the approximate solution for the population of the trapped hyperfine state

$$N_T(t)=\int d^3r\ \rho_0(\vec{r})\left\{\cos^2\left(\frac{\sqrt{\delta(\vec{r})^2+\omega_R^2}t}{2}\right)+\frac{\delta(\vec{r})^2}{\delta(\vec{r})^2+\omega_R^2}\sin^2\left(\frac{\sqrt{\delta(\vec{r})^2+\omega_R^2}t}{2}\right)\right\}^2, \qquad (6)$$

where $\rho_0(\vec{r})$ denotes the density distribution of the initial condensate and $\delta(\vec{r})\approx[m\omega^2(x^2+y^2)/2+m\omega_z^2z^2/2+mgz+\hbar\kappa(|\phi_{-1}|^2-|\phi_1|^2)/2]/\hbar$ is the spatially dependent detuning induced by the trapping magnetic field, the gravitational field, and the collective interatomic interaction. We see that if $\delta(\vec{r})=0$, Eq. (6) is identical to the resonant single-atom Rabi solution. The spatially dependent detuning $\delta(\vec{r})$ can account for the deviation of the experimental data from the single-atom resonant Rabi solution for small amplitudes of the rf pulse field. Generally speaking, the contribution from the collective interatomic interaction is time dependent and can be observed in the Rabi oscillation [22]. However, for the initial pencil-shaped condensate in the experiment of Mewes *et al.*, the gravitational potential is dominant over other terms [see Fig. 1(b)]. This is easily seen by the following numerical example. In terms of Refs. [4,17], the axial and the radical trapping frequencies for the trap are $\omega_z\sim 2\pi\times 18$ Hz and $\omega\sim 2\pi\times 320$ Hz, respectively. This leads to an axial length $z_0\sim 300$ μm and a radical width $r_0\sim 15$ μm for the pencil-shaped condensate. The peak density for the condensate $n_0\sim 3\times 10^{14}$ cm^{-3} and the interatomic interaction energy $n_0 4\pi\hbar^2 a/m\sim 385$ nK. By using these numerical values, we evaluate the gravitational potential with a magnitude ~ 8000 nK for sodium atoms, which is far larger than the interatomic interaction energy, the axial trapping potential $m\omega_z^2 z_0^2/2\sim 1582$ nK, and the radical trapping potential $m\omega^2 r_0^2/2\sim 1239$ nK. Hence the spatially dependent detuning due to the inhomogeneous gravitational field is the main reason for the fluctuations of the experimental data in the regime of the small amplitudes of the rf pulse. To further confirm our conclusion, we numerically calculate the Rabi oscillations for different lengths of the initial condensate in the axial direction. The results are shown in Fig. 3. We see that the longer the initial condensate, the larger the effect from the gravitational inhomogeneity, and the larger the deviation of the Rabi oscillations from the single-atom resonant solution. In addition we also see that the deviation can be reduced by increasing the amplitude of the rf pulse, which gives a large Rabi frequency. When the Rabi frequency is so large that the gravity-induced detuning can be ignored, the Rabi oscillations are approximately close to the resonant Rabi solution as shown in Fig. 3. On the other hand, for comparison, we plot the Rabi oscillations of the populations in the untrapped hyperfine states $m_F=0$ and $m_F=1$ in Fig. 4. Similarly the gravitational inhomogeneity has a large effect on the Rabi oscillations in the regime of the small amplitudes of the rf pulse.

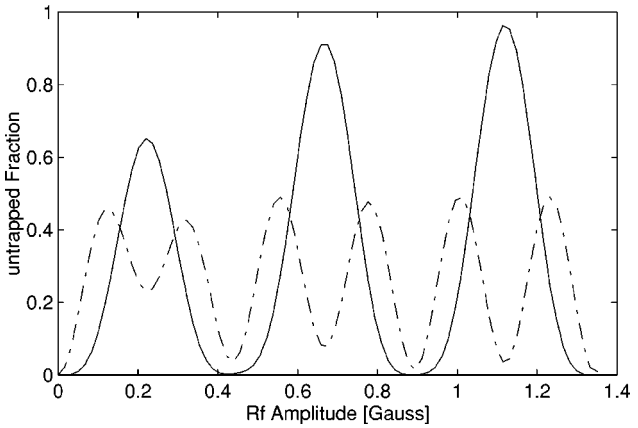

FIG. 4. The Rabi oscillations of the untrapped output condensate components: the dashed-dotted curve corresponds to $m_F=0$ and the solid curve to $m_F=1$.

So far we have studied the Rabi oscillations of the populations in the hyperfine states during the duration of the rf pulse. After the rf pulse has passed through the sample, the output condensate components will experience expansion and propagation, which is affected by both gravity and the collective interatomic interaction. To simulate the temporal-spatial evolution of the condensate components after the rf pulse, we must numerically solve the three-dimensional nonlinear coupled wave equations including the quantum dispersion due to the kinetic energy term. The three-dimensional simulation with nonlinear coupling is technically very difficult. However, in the present case with a pencil-shaped condensate gravity plays a dominant role in the motion of atoms in the axial direction over the interatomic interactions as discussed above. Hence we can seek approximately axial-radical separated solutions of Eqs. (4) with the forms $\psi_j(\vec{r},t)=\phi_j(x,y,t)u_j(z,t)$; $(j=-1,0,1)$. By ignoring the effect of the collective excitations on the motion of atoms in the axial direction, the wave functions $u_j(z,t)$ for different condensate components can approximately be determined by the single-atom Schrödinger equations with only gravitational and trapping potentials considered. In addition, considering the cylindrical symmetry of the initial condensate, we only need to simulate the expansion of radical wave functions due to the trapping potentials and collective interaction by reducing Eqs. (4) to two dimensions $(r\equiv\sqrt{x^2+y^2},t)$. The initial radical wave functions for this simulation are chosen to be the Rabi solutions excited by the rf pulse. The parameters used in the simulation are chosen to be the same as in the experiment of Mewes *et al.* To make a direct comparison with the experiment of Mewes *et al.*, we simulate the absorption imaging by using the numerically calculated density distributions. The absorption imaging directly reflects the expansion of the condensate components as shown in Fig. 5. Figure 5(a) corresponds to the image of the atomic cloud at $t=2$ ms after the rf pulse interaction. We see that the image is composed of three components. The sharp center line is the remaining condensate component in the trapped state $m_F=-1$, which overlaps with two output condensate components in untrapped states $m_F=0$ and $m_F=1$. The condensate component in state $m_F=1$ experiences a faster expansion than that in state $m_F=0$. This is due to the repelling force from the radical antitrapping potential in Eqs. (5). Numerical analysis shows that the radical width of the condensate in state $m_F=1$ exponentially depends on the radical trapping frequency ω and time t. The rapid ballistic expansion of the condensate in state $m_F=1$ results in a rapid decrease of the peak atomic density with time. As a result, the condensate component vanishes in the absorption image as shown in Fig. 5(b), which corresponds to the image of the cloud at $t=5$ ms. From Fig. 5(b) we see that the output condensate in state $m_F=0$ continues expanding due to the quantum dispersion and the collective interatomic interaction. In Figs. 5(c)–5(f), we simulate the dynamic expansion for longer times. These results show very similar features to those obtained in the experiment of Mewes *et al.* [17]. Our

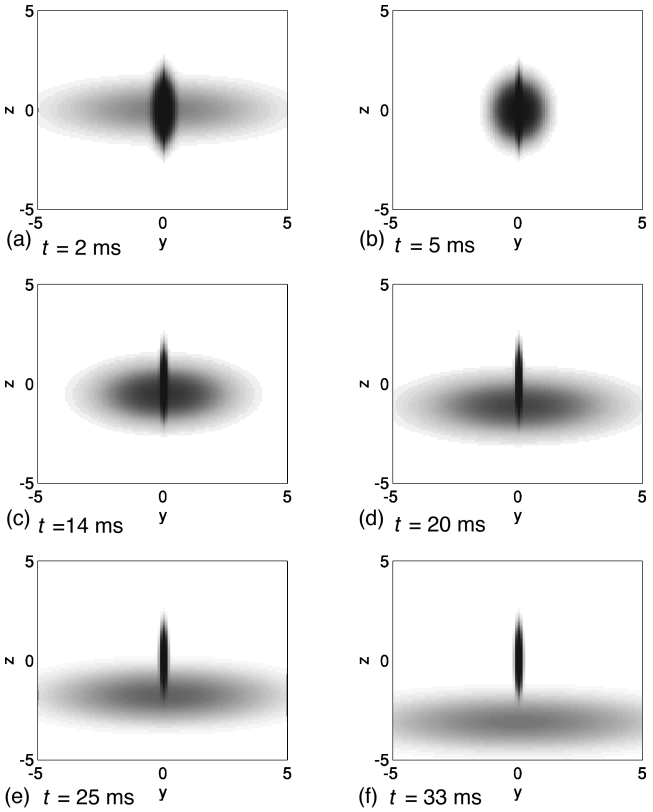

FIG. 5. The absorption imaging of the three-component condensate after the rf pulse interaction. The dynamic expansion of the atomic cloud quantitatively agrees with the experimental observation.

simulation also shows that the output condensate in state $m_F=0$ finally vanishes just as that in state $m_F=1$ due to the complete expansion. This case is similar to the propagation of a coherent optical pulse in free space. If one hopes to keep the output condensates for a longer propagating distance or longer time, one must employ some techniques such as atomic waveguide or laser beams to compress the expansion of the output condensates [15,16,23].

In conclusion, we have developed a nonlinear coupled wave theory for the interaction of the multicomponent coherent matter field with a rf field. We have applied this theory to study the Rabi oscillations and collective dynamics in the output coupler for Bose-condensed atoms demonstrated by Mewes *et al.* The numerical results quantitatively agree with the experiment. Furthermore the numerical simulations also reveal the roles played by gravity and the collective interatomic interaction in the output coupler.

The authors thank S. M. Tan, Craig Savage, and Muarry Olsen for their helpful discussions. W.Z. is grateful for the support of the Australian Research Council and the hospitality of the Physics Department of University of Auckland during his visit. D.F.W. is grateful for the support of the Marsden Fund of the Royal Society of New Zealand.

[1] M. Anderson *et al.*, Science **269**, 198 (1995).
[2] C. C. Bradley, C. A. Sackett, J. J. Tollet, and R. G. Hulet, Phys. Rev. Lett. **75**, 1687 (1995); **78**, 985 (1997).
[3] K. B. Davis *et al.*, Phys. Rev. Lett. **75**, 3969 (1995).
[4] M.-O. Mewes *et al.*, Phys. Rev. Lett. **77**, 416 (1996).
[5] D. S. Jin *et al.*, Phys. Rev. Lett. **77**, 420 (1996).
[6] M.-O. Mewes *et al.*, Phys. Rev. Lett. **77**, 988 (1996).
[7] B. Svistunov and G. Shlyapnikov, Zh. Eksp. Teor. Fiz. **97**, 821 (1990) [Sov. Phys. JETP **70**, 460 (1990)].
[8] H. D. Politzer, Phys. Rev. A **43**, 6444 (1991).
[9] M. Lewenstein and L. You, Phys. Rev. Lett. **71**, 1339 (1993).
[10] J. Javanainen, Phys. Rev. Lett. **75**, 1927 (1995).
[11] J. Javanainen and J. Ruostekoski, Phys. Rev. A **52**, 3033 (1995).
[12] R. Graham and D. F. Walls, Phys. Rev. Lett. **76**, 1774 (1996).
[13] A. Imamoglu and T. A. B. Kennedy, Phys. Rev. A **55**, R849 (1997).
[14] G. J. Milburn, J. Corney, E. M. Wright, and D. F. Walls, Phys. Rev. A **55**, 4318 (1997).
[15] Weiping Zhang, B. C. Sanders, and W. Tan, Phys. Rev. A **56**, 1433 (1997).
[16] S. Dyrting, Weiping Zhang, and B. C. Sanders, Phys. Rev. A **56**, 2051 (1997).
[17] M.-O. Mewes *et al.*, Phys. Rev. Lett. **78**, 582 (1997).
[18] Weiping Zhang and D. F. Walls, Phys. Rev. A **49**, 3799 (1994).
[19] Heping Zeng, Weiping Zhang, and Fucheng Lin, Phys. Rev. A **52**, 2155 (1995).
[20] R. J. Ballagh, K. Burnett, and T. F. Scott, Phys. Rev. Lett. **78**, 1607 (1997).
[21] E. Tiesinga *et al.*, Phys. Rev. A **46**, R1167 (1992).
[22] Weiping Zhang and Liu Quo-Qiang, Proc. SPIE **2995**, 240 (1997); Phys. Rev. B (to be published).
[23] Weiping Zhang, D. F. Walls, and B. C. Sanders, Phys. Rev. Lett. **72**, 60 (1994).